

Supplementary MATERIALS AND METHODS

Primary samples, cell lines, and culture conditions

Primary AML cells from peripheral blood and BM samples were obtained from 26 AML patients, and primary MSCs were obtained from healthy donor BM. Written informed consent was obtained in accordance with the requirements of The University of Texas MD Anderson Cancer Center's Institutional Review Board and the principles of the Declaration of Helsinki. The protocol was approved by the institutional ethics committees. Ficoll-Hypaque density gradient centrifugation was used to separate mononuclear cells (Sigma-Aldrich). MSCs were cultured at a density of 5000 to 6000 cells/cm² in minimum essential medium alpha supplemented with 20% fetal bovine serum, 1% L-glutamine, and 1% penicillin-streptomycin.

For coculture experiments, MSCs isolated at passage 2 or 3 comprising a single phenotypic population, as previously described,¹ were utilized. AML cell lines were cultured at a density of 5×10^5 /mL, with or without MSCs. AML cells were cocultured by plating them on top of MSCs and non-adherent AML cells were separated from the MSC monolayer by careful pipetting with ice-cold phosphate-buffered saline (PBS), repeated twice. The purity of the AML cells separated from MSCs was confirmed by the absence of *THY1* (*CD90*) mRNA expression as determined by polymerase chain reaction (PCR). After removing non-adherent AML cells, the AML cells adhered to co-cultured MSCs were trypsinized with MSCs (Thermo Fisher Scientific) and then separated from MSCs by magnetic-activated cell sorting (MACS) using anti-CD45 microbeads (Miltenyi Biotech).

In experiments comparing direct contact conditions to noncontact conditions, AML cells were plated in 12-well plates containing MSCs, either in direct contact or separated by a 0.4- μm porous transwell insert (Corning) that allowed passage of soluble growth factors.

Human OCI-AML3, MOLM13 and U937 cells were purchased from DSMZ. Cells were cultured in RPMI 1640 medium containing 10% heat-inactivated fetal bovine serum, 1% L-glutamine, 100 U/mL penicillin, and 100 $\mu\text{g}/\text{mL}$ streptomycin at 37 °C in a 5% CO₂ atmosphere. OCI-AML3 and MOLM13 cells were transduced with lentiviral vectors encoding a fusion of the mitochondrial localization sequence of a mitochondrial matrix enzyme, pyruvate dehydrogenase E1 alpha 1 (PDHA1) to the amino terminus of copGFP. MSCs were transduced with a lentiviral vector encoding a fusion of the same mitochondrial localization signal to the amino terminus of red fluorescent protein dsRed. The lentiviral expression vector was transfected using the X-treme GENE HP reagent (Sigma-Aldrich) according to the manufacturer's instructions. Three days after transfection, GFP-labeled cells were purified by fluorescence-activated cell sorting (Influx, Becton Dickinson).

Reagents

The OxPhos inhibitor IACS-010759² was obtained from the Institute for Applied Cancer Science at MD Anderson. Cytarabine was purchased from Wako Pure Chemical Industries. Cytochalasin D (Sigma-Aldrich), an ICAM-1 neutralizing antibody (Abcam), natalizumab (Biogen), dansylcadaverine (Wako), and bafilomycin (Sigma-Aldrich) were also used.

Analyses of cell viability and apoptosis

Cell viability and proliferation were assessed by using a Vi-Cell XR (Beckman-Coulter) cell counter using the trypan blue exclusion method or a CellTiter 96 AQueous One Solution Cell Proliferation Assay (MTS, Promega) according to the manufacturer's protocols. Apoptotic cell death was analyzed by annexin V/propidium iodide staining and flow cytometry as described elsewhere.³ For MSC coculture experiments, CD45 was used to distinguish MSCs (negative) from leukemia cells (positive). AML cells that adhered to MSCs were separated from cocultured MSCs by MACS using anti-CD45 microbeads after trypsinization. Apoptotic cell death of OCI-AML3 cells was detected by staining with annexin V-FITC/propidium iodide and a 1:100 dilution of anti-CD45 APC-conjugated antibody (BD Bioscience) by a FACScan flow cytometer (BD Bioscience).

ROS production

Total cellular ROS production was quantified by using the CellROX Deep Red Flow Cytometry Assay Kit, which contains SYTOX Dead Cell Stain (Life Technologies). Flow cytometric data were acquired using a FACScan flow cytometer and analyzed using FlowJo version 9.5 software (TreeStar).

Cap analysis gene expression

The cap analysis gene expression (CAGE) protocol was described previously; individual tag libraries were normalized by using the common power-law distribution approach.⁴ Expression data for annotated coding or noncoding genes (according to GencodeV10) were extracted by collecting normalized tag counts in regions from -500 to +200 relative to all annotated transcription start sites associated with a single gene ID. Normalized data were subjected to digital gene expression analysis by EdgeR and DEGseq,^{5,6} an R package for identifying differentially expressed genes. Then gene set enrichment analysis (GSEA)⁷ was performed to examine differences in promoter gene expression and functional networks.

Adhesion assay

Adhesion of AML cells was assessed by culturing them on MSCs for 48 hours at 37 °C in 5% CO₂, with or without IACS-010759 (30 nM). After coculture, AML cells suspended in the supernatant were removed. Adherent cells were detached by pipetting with PBS and counted after trypan blue exclusion staining of dead cells.⁸

Extracellular flux assays

The Seahorse XF24 Extracellular Flux analyzer (Seahorse Bioscience) was used to measure the oxygen consumption rate (OCR) of OCI-AML3, MOLM13, and U937 cells and MSCs according to the manufacturer's instructions.⁹ Briefly, AML cells were cultured with or without the indicated concentrations of IACS-010759 and/or an anti-ICAM-1

antibody in the presence or absence of MSCs for 2 hours. Before use in the extracellular flux assays, cocultured AML cells were separated from the MSC monolayer by careful pipetting. AML cells were counted, and 5×10^5 cells were added to each well for the extracellular flux assays. For MSCs, 6×10^4 cells were added to each well with or without IACS-010759 (30 nM) treatment for 2 hours. Three technical replicates for each condition were plated.

Immunoblot analysis

Immunoblot analysis was performed as previously described.³ LC-3 (MBL) and α -tubulin (Sigma-Aldrich) antibodies and horseradish peroxidase–linked anti-mouse and anti-rabbit IgG (Cell Signaling Technology) were used.

Confocal immunofluorescence assay

OCI-AML3 and MOLM13 cells² stably transfected with mitochondria-targeted *PDHA1*-GFP and/or MSCs transfected with *PDHA1*-dsRed were plated in cell culture dishes with glass bottoms and treated with the indicated reagents under the indicated conditions. Confocal fluorescence images were captured with Leica TCS-SP5 and Zeiss LSM780 confocal microscopes.

Assessment of mitochondrial transfer

Mitochondrial transfer was assessed by using a laser scanning confocal microscope or a FACScan flow cytometer. Briefly, OCI-AML3 and MOLM13 cells stably transfected

with mitochondria-targeted *PDHAI*-GFP or U937 cells, and MSCs transfected with *PDHAI*-dsRed were cocultured with the indicated treatment for the indicated time. Laser scanning was employed to obtain images from which the rate of mitochondrial transfer was quantitatively determined. The number of GFP and dsRed dual-positive OCI-AML3 and MOLM13 cells or dsRed-positive U937 cells per 100 GFP-positive cells ($n > 5$) was counted at 40 \times magnification by live-cell imaging with confocal microscopy as described elsewhere.¹⁰ For flow cytometric analysis, AML cells that adhered to MSCs were separated from cocultured MSCs by MACS using anti-CD45 microbeads after trypsinization. For MSC coculture experiments, a 1:100 dilution of anti-CD45 APC-conjugated antibody was added. CD45 was used to distinguish MSCs (negative) from leukemia cells (positive). Annexin V fluorescence was determined by a FACScan flow cytometer.

Mitophagy assay

To detect mitophagy, a Mitophagy Detection Kit (Dojindo Molecular Technologies) containing Mtpagy and Lyso dyes was used according to the manufacturer's instructions.¹¹ When mitophagy takes place, damaged mitochondria fuse to lysosomes, and Mtpagy dyes emit high fluorescence signals. The colocalization of Mtpagy and Lyso dyes was observed using a Leica TCS-SP5 confocal microscope.¹²

Analysis of mitochondrial membrane potential

JC-1 is a cell-permeant dye that can enter mitochondria and accumulate within them. Mitochondrial membrane potentials were measured by using a JC-1 Mitochondrial

Membrane Potential Assay Kit (Abcam) according to the assay protocol in the manufacturer's instructions. Polarized/energized mitochondria emit an orange-red fluorescence, and depolarized mitochondria emit green fluorescence. The fluorescence was analyzed with excitation/emission at 485/590 nm for mitochondrial polarization and at 485/525 nm for mitochondrial depolarization using a FLEX Station3 microplate reader (Molecular Devices). Mitochondrial depolarization was indicated by a decrease in the ratio of polarization to depolarization. The fluorescence of live cells was also observed using a BZ-X700 microscope (Keyence).

Electron microscopy and immunoelectron microscopy analysis

For electron microscopy analyses, cells were centrifuged at 14 000 rpm for 20 minutes, then cell pellets were fixed in 2% glutaraldehyde in 0.1 mol/L phosphate buffer (pH 7.4) for 1 hour at room temperature on a rocker. The pellets were rinsed in phosphate buffer, postfixed in 1% osmium tetroxide in phosphate buffer for 1 hour on ice, rinsed in buffer, and stabilized with a small amount of 2% agarose to hold them together. The pellets were then dehydrated through a graded series of ethanol to 100%, followed by QY1, and infiltrated with Epon resin (Oken Shoji) in a 1:1 solution of Epon:QY1 overnight on a rocker at room temperature. The next day, they were placed in fresh Epon for several hours and then embedded in Epon overnight at 60 °C. Thin sections were cut on a ultramicrotome (UC6, Leica Microsystems), collected on grids, stained with uranyl acetate and lead citrate, and examined under a Hitachi HT7700 transmission electron microscope.

To identify MSC-derived mitochondrial fragments inside autophagosomes in

cocultured AML cells, we performed immunogold staining of *PDHA1*-dsRed-transfected MSCs. For immunoelectron microscopy analysis, AML cells cocultured with *PDHA1*-dsRed transfected MSCs were fixed with 2% paraformaldehyde and 0.025% glutaraldehyde in 0.1 M phosphate buffer (pH 7.4), and embedded in LR white resin (Electron Microscopy Sciences). Sections were immunolabeled with a rabbit anti-dsRed antibody (MBL) and an anti-rabbit IgG 10 nm gold secondary antibody (BB International). This enabled detection of MSC-derived mitochondrial fragments stained by immunogold in cocultured AML cells.

Quantification of mitochondrial DNA copy number in vitro coculture system

A Human Mitochondrial DNA Monitoring Primer Set and Terra qPCR Direct TB Green Premix (Takara Bio) were used for quantitative PCR in conjunction with the Thermal Cycler Dice Real Time System Single (Takara Bio). mtDNA copy number was then determined according to the manufacturer's instructions. Real-time PCR was performed using a Model 7500 Real-time PCR System (Applied Biosystems).

***In vivo* mouse experiments for CAGE analysis**

Six- to-eight-week-old NOD-*scid* IL2R γ^{null} (NSG) mice ($n = 5$ for each model, from the Jackson Laboratory) were injected with 1 million AML patient-derived xenograft (PDX) cells (established at MD Anderson Cancer Center) 24 hours after exposure to 250 cGy irradiation. Four weeks after confirmation of engraftment in peripheral blood by hCD45⁺ flow cytometry, the mice were randomly assigned to receive IACS-010759 (5.0 mg/kg, 5 days on/2 days off) or vehicle (solvent-only control) by oral gavage ($n = 3$ in each

group). Sensitivity to IACS-010759 was defined by disease progression detected by engraftment (hCD45+ cells in circulation). PDXs in which treatment delayed engraftment by more than 3 weeks compared to vehicle were defined as sensitive. PDXs with no delay of 3 weeks or more were defined as resistant. Mice were sacrificed when full engraftment was detected by flow cytometry or when any sign of morbidity was observed. Spleen cells were collected and enriched for human cells by depleting mouse cells with an EasySep Mouse/Human Chimera Isolation Kit (Stem Cell Technologies) following the manufacturer's manual. The animal experiments were approved by The University of Texas MD Anderson Cancer Center's Institutional Animal Care and Use Committee.

Murine/human mtDNA quantification in the *in vivo* mouse model

Human primary AML cells were injected into NSG mice (1×10^6 cells per mouse). The ratio of murine to human mtDNA in spleen-resident AML cells in humanized AML PDX mouse models was examined after daily oral treatment with IACS-010759 (5.0 mg/kg/day, 5 days on/2 days off, 21 days) or vehicle. The Mouse Feeder Cell Quantification Kit (Takara Bio) was used to detect and quantify the mouse mtDNA copy number in engrafted AML cells. For normalization of the mouse mtDNA, human nuclear DNA and mouse nuclear DNA in the engrafted AML cells was quantified by real-time PCR using specific primers, Mouse_Mt_primer, Human_primer_Type II (CHR7), and Mouse_genome_primer, following the manufacturer's manual. Utilizing the standard curve of the CT values and the absolute amount of sample DNA, the ratio of mouse mtDNA / human nuclear DNA was calculated, then the difference of mtDNA ratio between IACS-

010759 and control was calculated. The negative value of mouse nuclear DNA was confirmed in AML cells.

Statistical analyses

GraphPad Prism 9 software was used for statistical analysis. All values are expressed as the mean \pm SD. Two-way ANOVA was used for comparisons of more than 2 groups. The Student *t*-test was used for 2-group comparisons. Differences were considered to be significant at $P < 0.05$.

Supplemental REFERENCES

1. Quinn TA, Camelliti P, Rog-Zielinska EA, et al. Electrotonic coupling of excitable and nonexcitable cells in the heart revealed by optogenetics. *Proc Natl Acad Sci U S A*. 2016;113(51):14852-14857.
2. Molina JR, Sun Y, Protopopova M, et al. An inhibitor of oxidative phosphorylation exploits cancer vulnerability. *Nat Med*. 2018;24(7):1036-1046.
3. Milella M, Kornblau SM, Estrov Z, et al. Therapeutic targeting of the MEK/MAPK signal transduction module in acute myeloid leukemia. *J Clin Invest*. 2001;108(6):851-859.
4. Takahashi H, Lassmann T, Murata M, Carninci P. 5' end-centered expression profiling using cap-analysis gene expression and next-generation sequencing. *Nat Protoc*. 2012;7(3):542-561.
5. Wang L, Feng Z, Wang X, Wang X, Zhang X. DEGseq: an R package for identifying differentially expressed genes from RNA-seq data. *Bioinformatics*. 2010;26(1):136-138.
6. Ohmiya H, Vitezic M, Frith MC, et al. RECLU: a pipeline to discover reproducible transcriptional start sites and their alternative regulation using capped analysis of gene expression (CAGE). *BMC Genomics*. 2014;15:269.
7. Subramanian A, Tamayo P, Mootha VK, et al. Gene set enrichment analysis: a knowledge-based approach for interpreting genome-wide expression profiles. *Proc Natl Acad Sci U S A*. 2005;102(43):15545-15550.

8. Gang EJ, Kim HN, Hsieh YT, et al. Integrin $\alpha 6$ mediates the drug resistance of acute lymphoblastic B-cell leukemia. *Blood*. 2020;136(2):210-223.
9. Vangapandu HV, Havranek O, Ayres ML, et al. B-cell Receptor Signaling Regulates Metabolism in Chronic Lymphocytic Leukemia. *Mol Cancer Res*. 2017;15(12):1692-1703.
10. Jiang D, Chen FX, Zhou H, et al. Bioenergetic Crosstalk between Mesenchymal Stem Cells and various Ocular Cells through the intercellular trafficking of Mitochondria. *Theranostics*. 2020;10(16):7260-7272.
11. Konig J, Ott C, Hugo M, et al. Mitochondrial contribution to lipofuscin formation. *Redox Biol*. 2017;11:673-681.
12. Kameyama K, Motoyama K, Tanaka N, Yamashita Y, Higashi T, Arima H. Induction of mitophagy-mediated antitumor activity with folate-appended methyl-beta-cyclodextrin. *Int J Nanomedicine*. 2017;12:3433-3446.

Fig S1

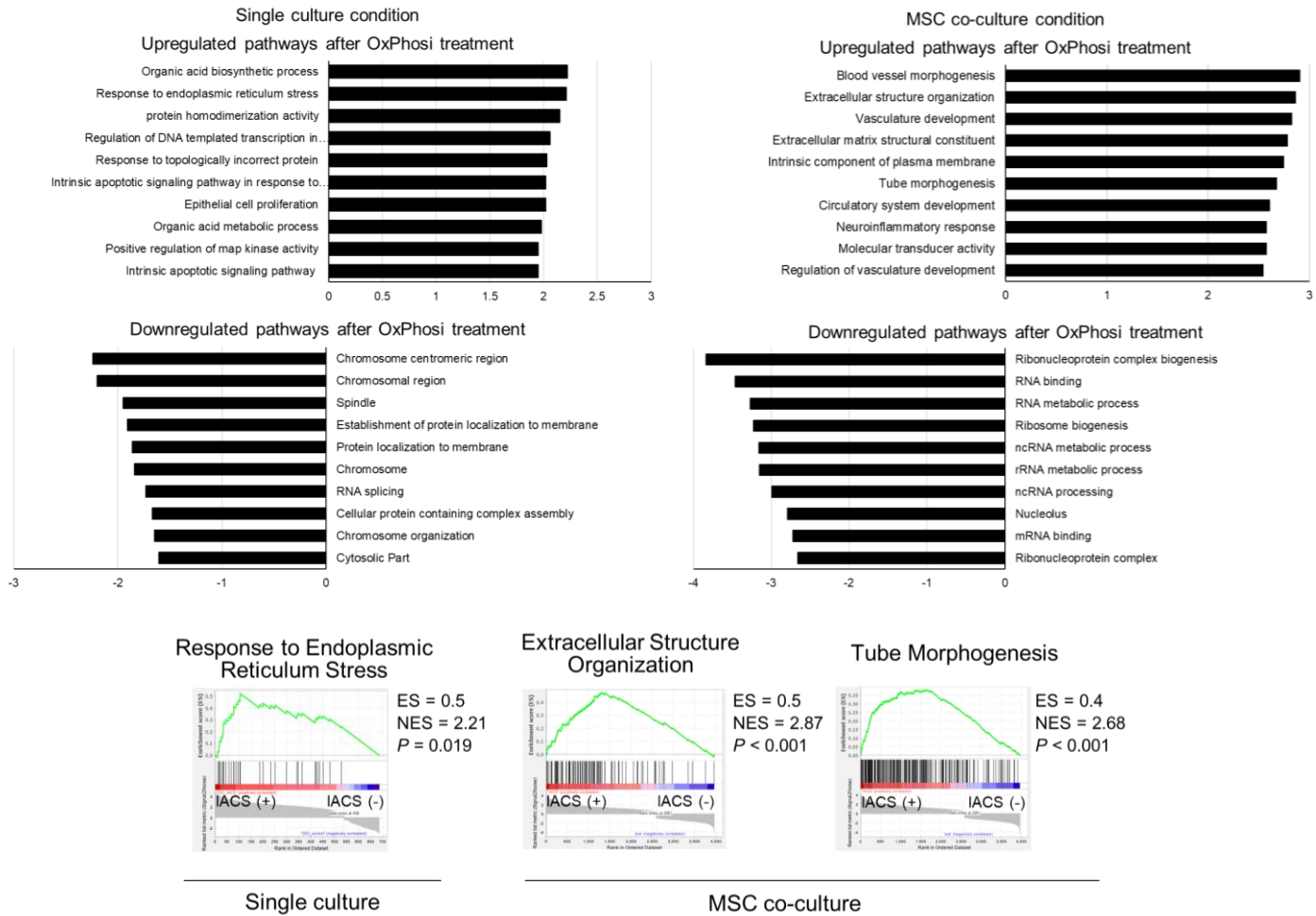


Fig S2

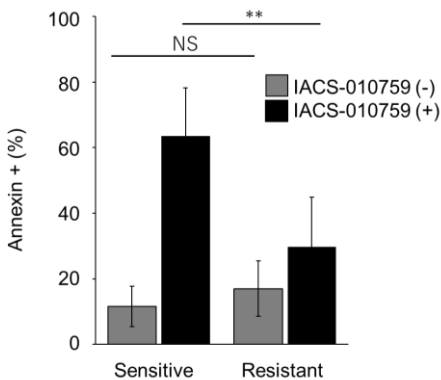


Fig S3

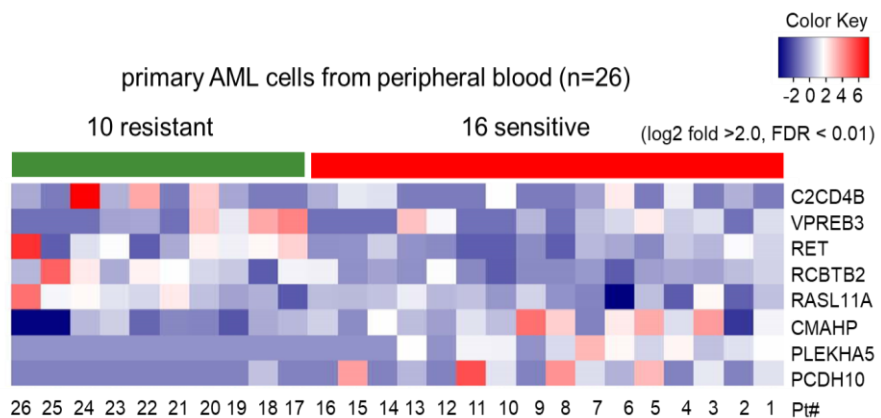


Fig S4

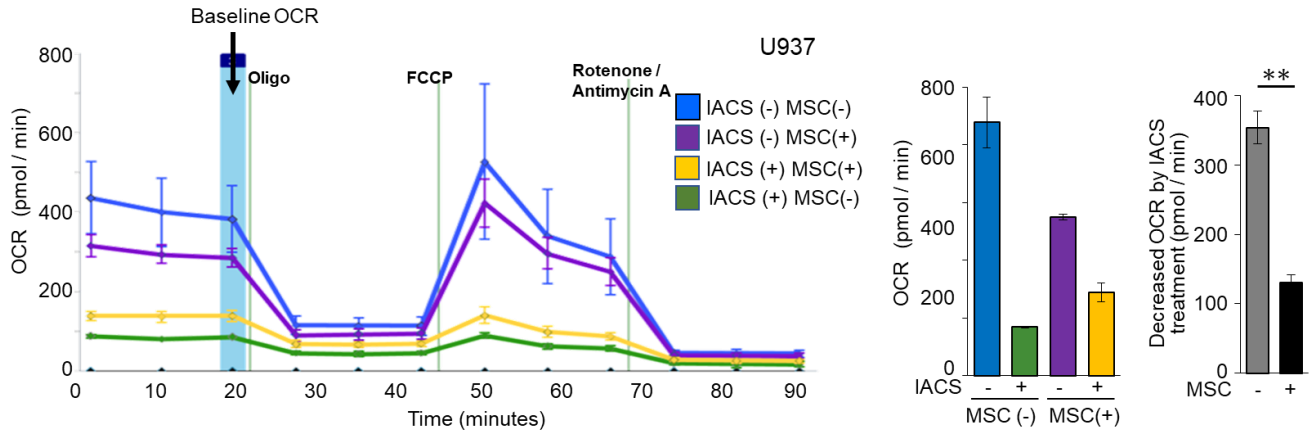


Fig S5

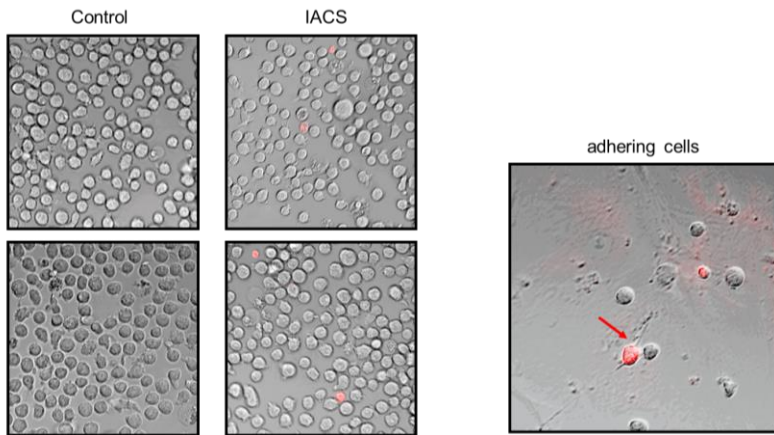


Fig S6

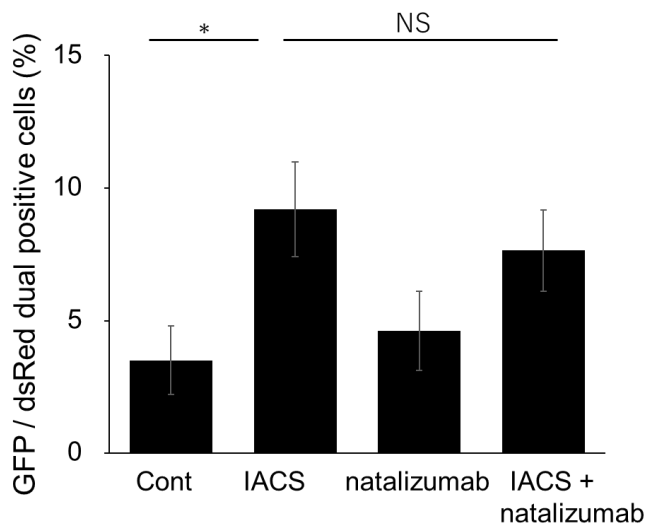


Fig S7

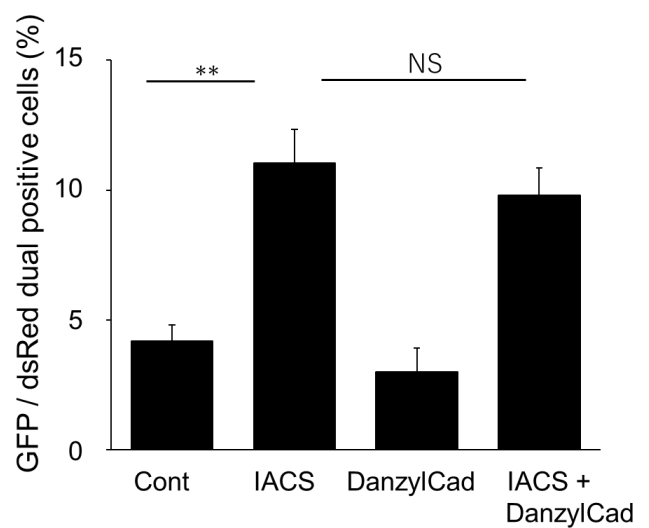


Fig S8

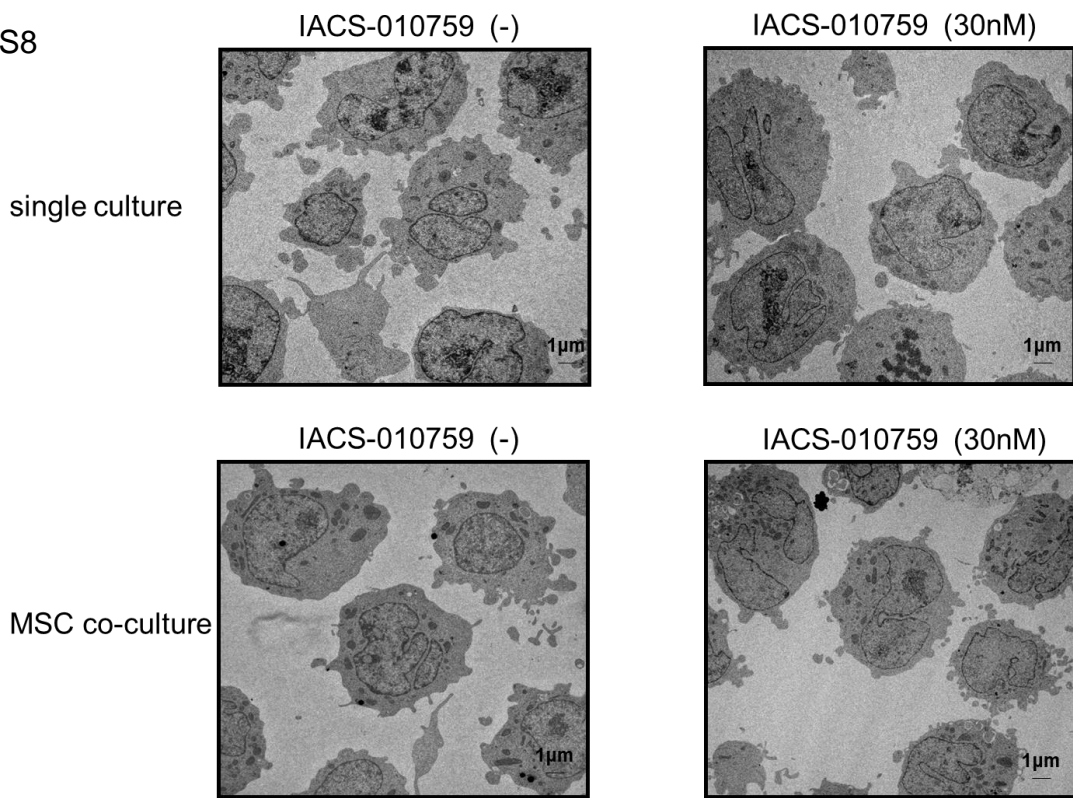
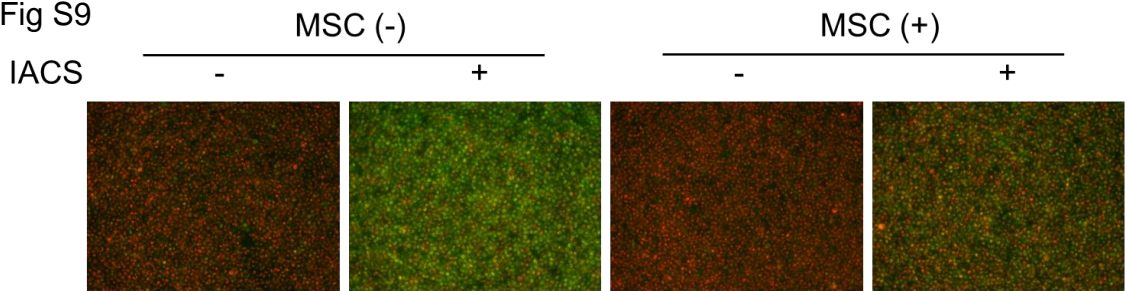


Fig S9



aggregated JC-1(red) / monomer JC-1 (green) merged

Fig S10

